ORIGINAL RESEARCH

Intravascular Stem Cell Bioreactor for Prevention of Adverse Remodeling After Myocardial Infarction

Peter V. Johnston, MD;* Chao-Wei Hwang, MD, PhD;* Virginia Bogdan; Kevin J. Mills, MD; Elliott R. Eggan, MD; Aleksandra Leszczynska, PhD; Katherine C. Wu, MD; Daniel A. Herzka, PhD; Jeffrey A. Brinker, MD; Steven P. Schulman, MD; Monisha Banerjee, MD; Victoria Florea, MD; Makoto Natsumeda, MD; Bryon Tompkins, MD; Wayne Balkan, PhD; Joshua M. Hare, MD; Gordon F. Tomaselli, MD; Robert G. Weiss, MD; Gary Gerstenblith, MD

***Background*—**Prevention of adverse remodeling after myocardial infarction (MI) is an important goal of stem cell therapy. Clinical trial results vary, however, and poor cell retention and survival after delivery likely limit the opportunity to exert beneficial effects. To overcome these limitations, we built an implantable intravascular bioreactor (IBR) designed to protect contained cells from washout, dilution, and immune attack while allowing sustained release of beneficial paracrine factors.

***Methods and Results*—**IBRs were constructed using semipermeable membrane adhered to a clinical-grade catheter shaft. Mesenchymal stem cell (MSC) viability in and paracrine factor release from IBRs were assessed in vitro and IBR biocompatibility and immune protection confirmed in vivo. In a porcine anterior MI model, IBRs containing 25 million allogeneic MSCs (IBR-MSCs) were compared with IBRs containing media alone (IBR-Placebo; n=8 per group) with adverse remodeling assessed by magnetic resonance imaging. Four weeks after MI, IBR-MSCs had no significant change in end-diastolic volume (+0.33±4.32 mL; *P*=0.89), end-systolic volume (+2.14±4.13 mL; *P*=0.21), and left ventricular ejection fraction (−2.27±2.94; *P*=0.33) while IBR-Placebo had significant increases in end-diastolic volume (+10.37±3.84 mL; *P*=0.01) and ESV (+11.35±2.88 mL; *P*=0.01), and a significant decrease in left ventricular ejection fraction (−5.78±1.70; *P*=0.025). Eight weeks after MI, adherent pericarditis was present in 0 of 8 IBR-MSCs versus 4 of 8 IBR-Placebo (*P*=0.02), suggesting an anti-inflammatory effect. In a separate study, 25 million allogeneic pig MSCs directly injected in the peri-infarct zone 3 days after MI (n=6) showed no significant benefit in adverse remodeling at 4 weeks compared with IBR-MSCs.

***Conclusions*—**MSCs deployed inside an implantable, removable, and potentially rechargeable bioreactor in a large animal model remain viable, are immunoprotected, and attenuate adverse remodeling 4 weeks after MI. **(*J Am Heart Assoc*. 2019;8:e012351. DOI: 10.1161/JAHA.119.012351.)**

Key Words: cytokines • growth factors • myocardial infarction • remodeling heart failure • stem cell

Administration of stem cells following myocardial infarction (MI) promotes regeneration of cardiac tissue, decreases inflammation-associated cell loss, and thereby limits adverse remodeling, which is associated with the subsequent development of heart failure and associated morbidity and mortality.[1,2] The effects of stem cell administration on adverse remodeling in many clinical trials, however, are modest.[3–6] One reason may be that only a small percentage of cells delivered to the heart using current methods remain there, and of those that do, few survive for any significant time.[7,8] There is growing evidence from preclinical studies that many of the positive effects of stem cell therapy result from their release of growth factors and cytokines, collectively referred to as "paracrine factors" (PFs), which enhance endogenous repair mechanisms and reduce maladaptive inflammation and apoptosis after tissue

From the Division of Cardiology, Departments of Medicine (P.V.J., C.-W.H., V.B., A.L., K.C.W., J.A.B., S.P.S., R.G.W., G.G.) and Biomedical Engineering (C.-W.H., D.A.H.), Johns Hopkins University School of Medicine, Baltimore, MD; Albert Einstein College of Medicine, Bronx, NY (G.F.T.); Department of Medicine, Penn State Hershey Medical Center, Hershey, PA (K.J.M.); Perelman School of Medicine, University of Pennsylvania, Philadelphia, PA (E.R.E.); Interdisciplinary Stem Cell Institute (M.B., V.F., M.N., B.T., W.B., J.M.H.), Departments of Surgery (M.B., B.T.) and Medicine (W.B., J.M.H.), University of Miami Miller School of Medicine, Miami, FL.

*Dr Johnston and Dr Hwang contributed equally to this work.

Correspondence to: Peter V. Johnston, MD, Division of Cardiology, Department of Medicine, Johns Hopkins University School of Medicine, Ross Building #1167, 720 Rutland Avenue, Baltimore, MD 21287. E-mail: pjohnst1@jhmi.edu

Received May 2, 2019; accepted July 5, 2019.

Clinical Perspective

What Is New?

- This study tested a novel intravascular bioreactor that was designed to house a large number of stem cells in a protected space within the body and allow free release of soluble paracrine factors (growth factors, cytokines, etc), but not of cells, and in doing so to determine whether this method could limit adverse remodeling after myocardial infarction in a large animal model.

What Are the Clinical Implications?

- The results of this study indicate that it is not necessary to directly inject stem cells in the heart to elicit a beneficial effect and suggest a new method by which adverse remodeling after myocardial infarction, which is known to be an important pathologic mechanism in the development of heart failure, may be prevented or reduced.

injury.[9–12] It follows that if cells delivered to the heart remain there and survive for only a limited period, the time opportunity for the cells to exert beneficial effects via paracrine mechanisms is limited as well.[3,8]

To increase the time exogenous stem cells can survive and exert beneficial paracrine-mediated effects, we developed an implantable bioreactor (IBR). The device houses a population of exogenous stem cells in the vascular space within a semipermeable pouch that allows for free exchange of PFs, nutrients, and waste but not of cells. By preventing stem cell escape and host immune cell entry, the IBR provides a protected environment within which contained cells survive for an extended period in vivo, thus allowing for a prolonged time opportunity for the release of beneficial PFs to limit adverse remodeling.

Here, we report a proof-of-concept study using a catheter-based IBR deployed in the venous vasculature. Biocompatibility of, and immunoprotection afforded by, the IBR were assessed with the device deployed in the superior vena cava in farm pigs. In a subsequent placebo-controlled preclinical MI study, the effects of IBRs containing mesenchymal stem cells (MSCs) on magnetic resonance imaging (MRI)-assessed changes in cardiac volumes, ejection fraction, and late gadolinium enhancement (LGE) were compared with those of placebo IBRs 4 weeks after anterior MI. In a separate experiment, the effects of direct injection (DI) of the same number of MSCs in the peri-infarct zone on adverse remodeling were also assessed. In addition to testing a novel device, these experiments also tested the "paracrine hypothesis" that the beneficial effects of stem cells on the heart are mediated to a significant extent by paracrine mechanisms.

Methods

Data and study materials will be made available to other researchers for purposes of reproducing the results or replicating the procedures. Interested researchers may contact the corresponding author.

MSC Isolation and Culture

The in vitro and the preliminary in vivo IBR experiments were conducted using human bone marrow–derived MSCs (hMSCs; Lonza, Walkersville, MD). The in vivo study of IBR therapy in MI was conducted using bone marrow–derived porcine MSCs (pMSCs) isolated from bone marrow aspirates of Yorkshire swine (15–20 kg) using established techniques.[13–15] The pMSCs were analyzed for expression of MSC-specific surface markers including CD90, CD44, CD34, and CD45 using a BD LSRII flow cytometer (BD Biosciences, San Jose, CA). Data were gated and analyzed using FlowJo software (Tree Star, Ashland, OR). Osteogenic and adipogenic differentiation assays were performed as described previously.[16] Briefly, pMSCs were plated in 6-well plates at 30 000 cells/well (osteogenic assay) and 200 000 cells/well (adipogenic assay). On day 1, cells were treated with specific induction media. For the osteogenesis assay, the media were changed every 3 days, and calcium deposition was quantified at 2 weeks. For the adipogenesis assay, lipid accumulation was quantified following 3 cycles of induction and maintenance as described previously.[17]

Media

In culture, both hMSCs and pMSCs were grown in media composed of: Alpha-MEM (Mediatech, Manassas, VA) supplemented with 20% fetal bovine serum (Hyclone, Logan, UT), L-glutamine (350 μg/mL; Mediatech), and penicillin/streptomycin (50 IU/mL/50 μg/mL; Corning Mediatech, Manassas, VA). These media were used for all experiments, including in vitro assessment of PF release and in vivo testing of IBR biocompatibility and postinfarction efficacy.

Bioreactor Construction

The IBR (Figure 1) was constructed from a semipermeable cellulose ester membrane with a molecular weight cutoff of 100 kDa (Spectrum Labs, Rancho Dominguez, CA). A 10-cm membrane segment was attached to a 20-cm modified 6-French vascular catheter (Boston Scientific, Marlborough, MA) with a heat-sealed distal end and the shaft fenestrated at 1-cm intervals using an 18-gauge needle. The membrane was secured to the midportion of the modified catheter using cyanoacrylate medical device adhesive (Henkel, Rocky Hill,

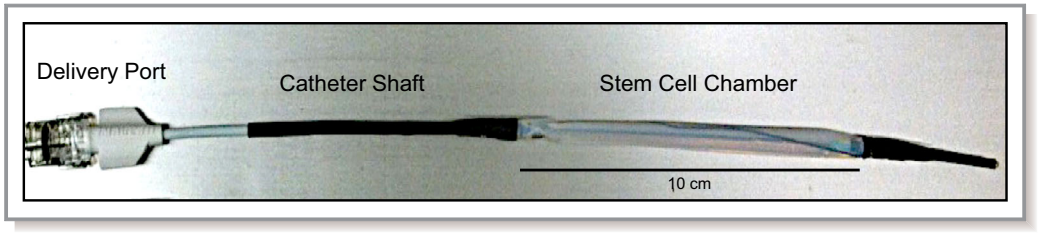

Figure 1. Implantable bioreactor (IBR) prototype. The cell suspension is injected into the delivery port, which is connected to the polymeric semipermeable stem cell chamber via a clinical-grade vascular catheter shaft.

CT), 2-0 silk surgical suture, and 0.125-inch medical grade heat shrink tubing (InsulTab, Woburn, MA). IBRs were sterilized in 70% ethanol under ultraviolet light for 12 hours and washed in phosphate-buffered saline (Corning Mediatech) and media before cell culture experiments and in vivo implantation.

In Vitro IBR PF Release

To assess in vitro PF release, IBRs were loaded with increasing numbers of hMSCs (10^5, 10^6, 5×10^6) and submerged in media in separate flasks for 7 days under standard mammalian cell culture conditions (37°C, 5% CO_2). Samples of media outside the IBRs were collected on days 1, 3, and 7; centrifuged to pellet any debris; and then flash frozen at −80°C. Concentrations of vascular endothelial growth factor (VEGF), basic fibroblast growth factor, hepatocyte growth factor, and interleukin-8 in IBR-conditioned media (CM) were assessed using multiplex ELISA (Quansys, Logan, UT). Bioreactors loaded with media alone (ie, no cells) were used as controls. At 7 days, hMSCs recovered from IBRs underwent viability assessment by Trypan Blue exclusion. To assess PF-release dose response, 6 additional CM experiments were conducted with IBRs loaded with 10^7, 2.5×10^7, and 4.5×10^7 hMSCs. Samples of CM collected from outside the IBRs on days 1, 3, and 7 were assessed for VEGF production by ELISA (R&D Systems, Minneapolis, MN).

In Vivo Biocompatibility and Immune Protection

To assess IBR biocompatibility and immune protection in vivo, IBRs containing 10^6 hMSCs (ie, xenogeneic) were inserted in the right internal jugular vein in Yorkshire swine (20–30 kg) via surgical cutdown and advanced to the junction of the superior vena cava and right atrium under fluoroscopic guidance (n=2). Animals were assessed daily for 1 week for fever, hemodynamic compromise, and dermatologic reaction that would suggest acute rejection. After 7 days, IBRs were removed, washed with sterile phosphate-buffered saline, and immediately submerged in media and placed in culture. As previously done, samples of CM from outside the IBRs were collected at days 1, 3, and 7, and the concentrations of PFs measured via multiplex ELISA. After 7 days in culture, hMSCs recovered from the IBRs were plated on standard tissue culture flasks to assess morphology and growth.

Preclinical Model of MI

Anterior MI was produced in female Yorkshire swine (20–30 kg) using 90-minute catheter-based balloon occlusion of the mid–left anterior descending artery as previously described (n=22).[18,19]

Baseline MRI

Three days after MI, baseline cardiac MRI with LGE was performed using a whole-body 3.0 T magnetic resonance scanner to assess left ventricular function, end-diastolic volume (EDV), end-systolic volume (ESV), and LGE before implantation of an IBR. Cine images were acquired using a radiofrequency spoiled gradient recalled echo pulse sequence (repetition time, 4.3 ms, echo time, 2.1 ms; flip α=12°; in-plane resolution 1.3×1.3 mm; 30 phases/cardiac cycle). Images for LGE were acquired after peripheral injection of Magnevist 0.2 mmol/kg (Bayer, Wayne, NJ) with an inversion recovery–prepared T1-weighted gradient echo sequence (repetition time, 5.3 msec; echo time, 2.6 msec; 1 R-R interval; flip α=20°; in-plane resolution 1.4×1.5 mm). Short-axis images from base to apex were acquired with 6-mm slice thickness and no gap for cine and LGE images.

Bioreactor Implantation

After baseline MRI, surgical cutdown of the right neck was performed to isolate the internal jugular vein, and an IBR was inserted as described above. Animals were randomly assigned to an IBR loaded with (1) 2.5×10^7 allogeneic pMSCs suspended in media (IBR-MSC), or (2) media alone (IBR-Placebo; n=8 both groups). For the IBR-MSC group, allogeneic pMSCs at passages 3 to 6 were harvested, counted, and assessed for viability by Trypan Blue exclusion immediately before loading. A total of 2.5×10^7 viable pMSCs were

suspended in media to a volume of 1.5 mL for infusion into the IBR, followed by 0.5 mL of media to flush cells into the cell chamber. Placebo IBRs were loaded with 2 mL of media alone. Once loaded, the IBR infusion port was closed with a sterile cap, the proximal shaft secured in place with suture, and the wound closed. Animals were then followed for any sign of immune reaction, rejection, or wound dehiscence.

Four-Week MRI and IBR Removal

Four weeks later, repeat cardiac MRI was performed using the same parameters, followed by surgical cutdown to expose and remove the IBR. Explanted IBRs were washed in sterile phosphate-buffered saline, placed in culture flasks submerged in culture medium (175 mL), and maintained in culture for 7 days. CM collected from outside the IBRs on days 1, 3, and 7 were assessed for VEGF release by ELISA for human VEGF (R&D Systems), which is known to cross react with porcine VEGF.[20]

Eight-Week MRI, Hemodynamic Assessment, and Necropsy

A final MRI was performed 4 weeks after IBR removal, that is, 8 weeks after MI. After MRI, invasive hemodynamic assessment was performed using a solid-state transducer (Millar, Houston, TX) followed by coronary angiography. Animals were then euthanized and necropsy performed with removal and inspection of the heart and pericardium, as well as other vital organs (lungs, liver, spleen, and kidneys). Sections of heart tissue were stained with hematoxylin and eosin or Masson's trichrome to assess scar and vasculogenesis at the infarct border zone.

MRI Image Analysis

MRI images were analyzed using Cinetool (GE Healthcare, Milwaukee, WI) by 2 observers blinded to the group assignment. When present, LGE was quantified as dense "core" and heterogeneous peri-infarct "gray zone" extents using previously published methods.[21,22] The core zone was composed of all pixels with signal intensity (SI) >50% of maximal SI within the region of LGE. Gray zone extent comprised all pixels with SI greater than peak SI in normal myocardium, but <50% of maximal SI within the hyperenhanced region. Total infarct size was defined as the sum of the "core" and "gray zone" extents.

Comparison Study of Intramyocardial DI of MSCs

To assess the impact of delivery of the same number of pMSCs (2.5×10^7) to the heart via intramyocardial injection, a separate group of animals (n=6) underwent anterior MI induced using the same protocol.[18,19] Three days later, cardiac MRI with LGE was performed, followed by DI of allogeneic pMSCs in the MI border zone using the NOGA Myostar injection-catheter system as previously described.[23] Briefly, the mapping catheter was advanced through a 9-French introducer sheath and retrograde across the aortic valve. A complete map of left ventricular geometry and function was generated by collecting local position and electrocardiographic data at >50 points in the endocardium. A viable infarct border zone was determined as a unipolar voltage from 6 to 12 mV. A total of 25 million viable pMSCs, divided into 10 injections, each 0.5 mL in volume, were delivered to the endocardium of the border zone. Injection sites were recorded both in the electroanatomic NOGA map and in 2 orthogonal radiographic projections and marked on a tracing of the endocardial silhouette. Animals receiving DI MSCs were followed for 8 weeks using the same MRI LGE imaging protocol as outlined above with results interpreted by readers blinded to the experimental procedure.

All animal experiments were performed under a protocol approved by either the Johns Hopkins University Animal Care and Use Committee (#SW10M468; IBR experiments) or the University of Miami (#14-193; DI experiment).

Statistical Analysis

All data are reported as mean± SEM. Analyses of paired data were performed using the Wilcoxon signed-rank test and unpaired data using the Wilcoxon rank-sum (Mann–Whitney) test. For ratios, outcomes were compared using the Fisher exact test. For comparisons across the 3 groups, analyses were performed with the Kruskal–Wallis rank test with Dunn's test for post hoc analyses. A P value of ≤0.05 was deemed statistically significant.

Results

In Vitro PF Release

Human MSCs grown in IBRs in vitro showed high viability after 7 days in culture (mean, 75.4±11.6%; n=6). The majority of MSCs adhered to the inner wall of the IBR cell chamber. When 10^6 hMSCs were housed in an IBR, there was release of relevant PFs, including VEGF, hepatocyte growth factor, basic fibroblast growth factor, and interleukin-8 over 7 days in culture (n=6; Figure 2A). To determine the dose of MSCs used in the in vivo studies, a dose-response experiment performed using escalating doses of hMSCs over 7 days in culture showed VEGF production increased to a dose of 2.5×10^7 cells (Figure 2B). There was no further increase in VEGF production when the IBR was loaded with a higher

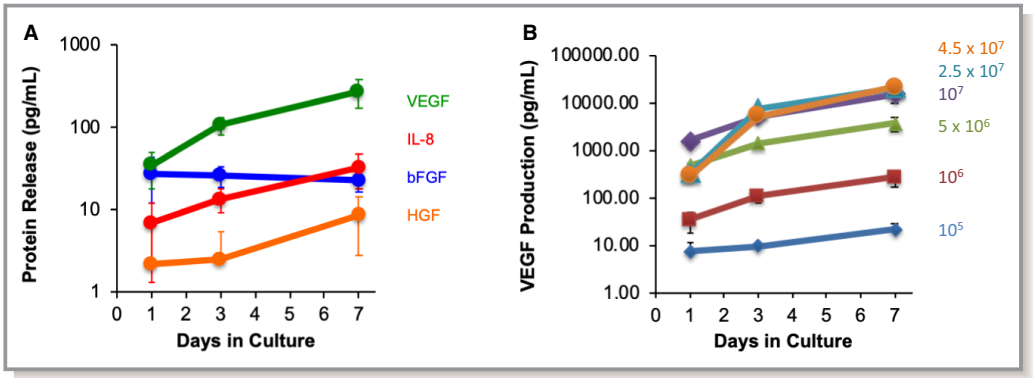

Figure 2. Paracrine factor release from implantable bioreactor (IBR) in vitro. Assessment of conditioned media collected from outside IBRs containing 10^6 human mesenchymal stem cells (MSCs) over 7 days in culture showed production and release of vascular endothelial growth factor (VEGF; green), interleukin 8 (IL-8; red), basic fibroblast growth factor (bFGF; blue), and hepatocyte growth factor (HGF; orange) as assessed by multiplex ELISA (**A**; log scale; n=6). A subsequent dose-finding experiment using IBRs loaded with increasing doses of hMSCs showed dose-dependent VEGF production up to a dose of 2.5×10^7 MSCs (**B**; log scale; n=6).

number of cells; hence, the dose of 2.5×10^7 was chosen for the preclinical MI experiment.

In Vivo Biocompatibility and Immune Protection

To determine whether the IBR was biocompatible and afforded immune protection for contained cells, devices were implanted in adult pigs and loaded with 10^6 hMSCs (Figure 3A). Despite use of xenogeneic hMSCs, there was no evidence of immune or transfusion reaction. After 1 week in vivo, the IBRs were removed and placed in culture. Analysis of CM collected over the subsequent 7 days showed continued production and release of relevant PFs (Figure 3B). Cells recovered from the IBRs were plated and showed continued growth and division with normal MSC morphology (Figure 3C).

Porcine MSC Isolation and Characterization

For the preclinical MI experiments, pMSCs were isolated from bone marrow biopsies obtained from Yorkshire swine. Assessment of surface marker expression confirmed MSC phenotype with markers typical of MSCs: $CD90^+$ and $CD44^+$; $CD34^-$ and $CD45^-$ (Figure 4A). Isolated pMSCs also showed typical osteogenic (Figure 4B) and apidogenic differentiation (Figure 4C). The pMSCs used for the study were low passage

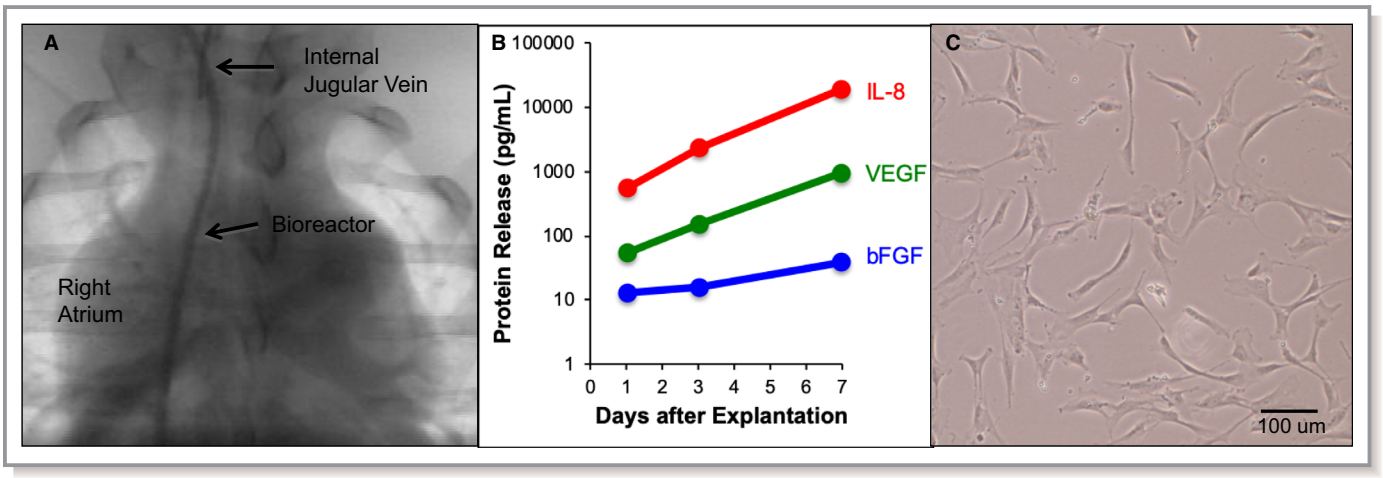

Figure 3. Biocompatibility testing and human mesenchymal stem cell (MSC) survival in implantable bioreactor (IBR) implanted in pigs. IBR implanted via neck with catheter shaft in right internal jugular vein and stem cell chamber at the level of the right atrium (**A**). Human MSCs recovered from IBR after 1 week in vivo (n=2) show continued production of basic fibroblast growth factor (bFGF; blue), vascular endothelial growth factor (VEGF; green), and interleukin 8 (IL-8; red) by multiplex ELISA (**B**), as well as normal MSC morphology (**C**).

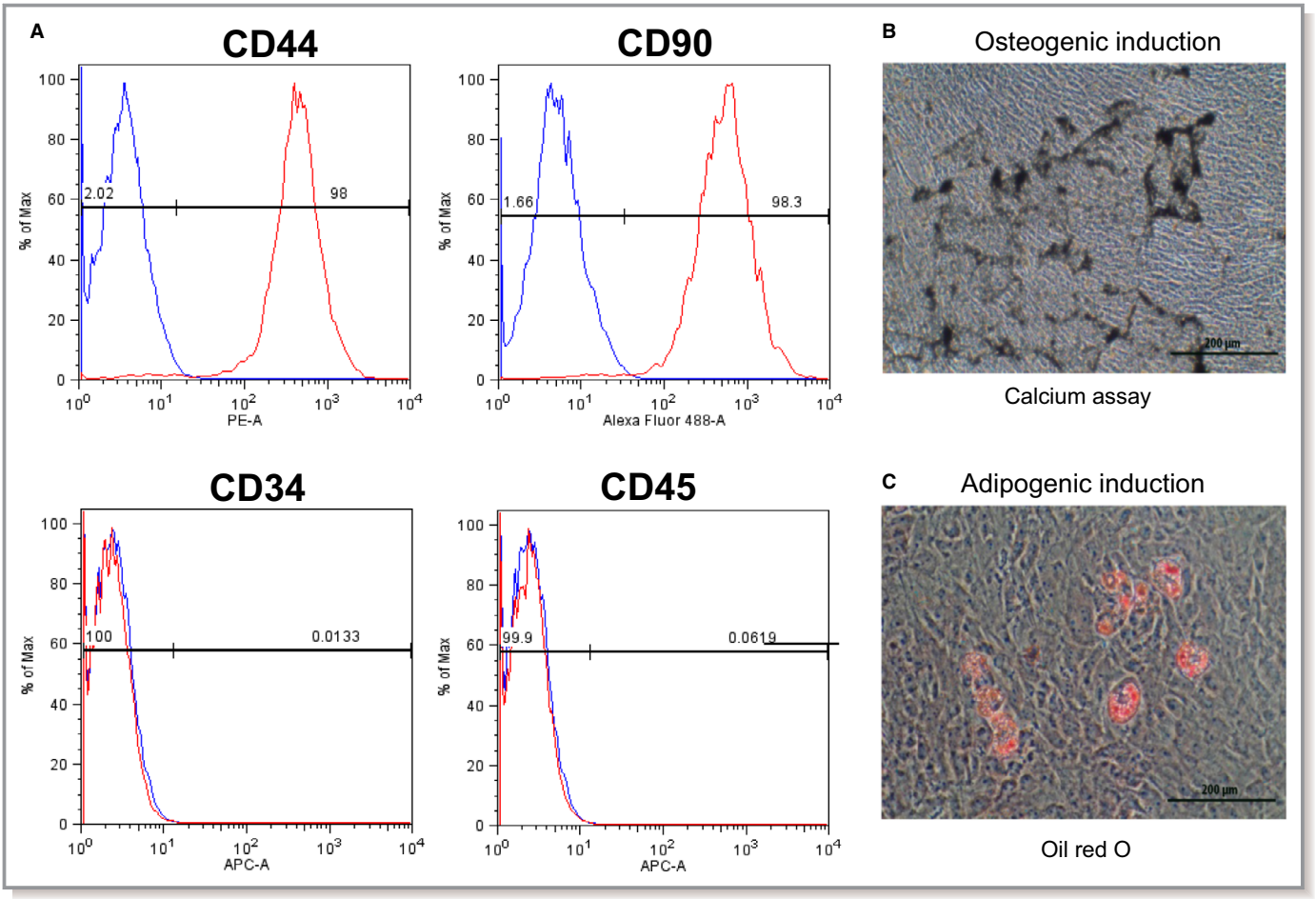

Figure 4. Porcine mesenchymal stem cells (MSCs) characterized by flow cytometry were $CD44^{+}$, $CD90^{+}$, $CD34^{-}$, and $CD45^{-}$, consistent with MSC phenotype (**A**). In addition, porcine MSCs showed typical osteogenic and apidogenic differentiation, as assessed by calcium deposition (**B**), and lipid accumulation (**C**), respectively.

(mean passage, 3.8±1.0) with high viability (mean viability, 98.8±0.6%) at preparation.

Placebo-Controlled Preclinical IBR MI Study

For the randomized IBR study (Figure 5), MI was induced in 22 pigs, 16 (74%) of which survived to the baseline MRI performed 3 days later. Baseline MRI on these 16 animals showed large anteroapical infarcts involving 28.9±9.7% of the left ventricle by mass and significant systolic dysfunction with mean left ventricular ejection fraction (LVEF) of 44.6±9.1%. There were no significant differences on baseline MRI between the 2 groups in terms of infarct size, LVEF, EDV, or ESV (Table). After baseline MRI, an IBR was implanted and loaded with 2.5×10^{7} pMSCs (IBR-MSC group) or media alone (IBR-Placebo). Bioreactor implantation was well tolerated and without complication. No animals showed evidence of immune rejection or transfusion reaction over the 4 weeks the IBRs remained implanted.

Week 4 Cardiac MRI

Repeat cardiac MRI at 4 weeks after implantation in the IBR-MSC group showed no significant changes in EDV (+0.33±4.32 mL; *P*=0.89), ESV (+2.14±4.13 mL; *P*=0.21), or LVEF (−2.27±2.94%; *P*=0.33) compared with baseline. In contrast, there were significant increases in both EDV (+10.37±3.84 mL; *P*=0.01) and ESV (+11.35±2.88 mL; *P*=0.01), as well as a significant decrease in LVEF (−5.78±1.70%; *P*=0.025) in the IBR-Placebo group (Figure 6). These changes in the IBR-Placebo group are consistent with pathologic left ventricular remodeling typical after large infarcts. On comparison between the groups, the change in ESV was significantly lower in the IBR-MSC group than in the IBR-Placebo group (*P*=0.036), although not the change in EDV (*P*=0.059). There was no significant difference between the groups for the change in LVEF (*P*=0.40).

The total infarct extent, as assessed as the sum of the core and gray zone masses by LGE decreased significantly 4 weeks after MI in both the IBR-MSC group (−3.99±1.62 g; *P*=0.049)

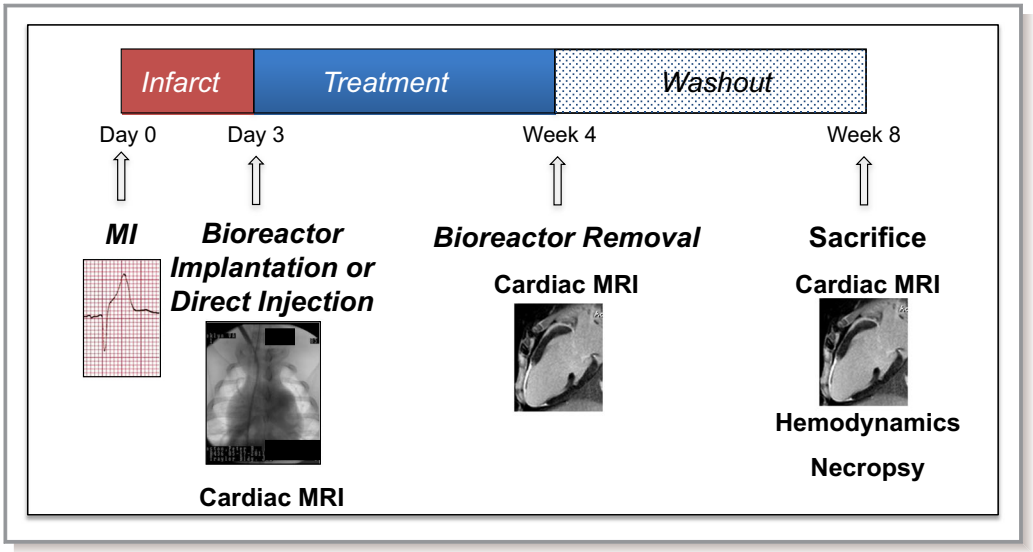

Figure 5. Schematic of the preclinical MI study. Three days after myocardial infarction (MI), farm pigs underwent late gadolinium-enhanced magnetic resonance imaging (MRI) followed by (1) implantation of an implantable bioreactor (IBR) loaded with 2.5×10^7 allogeneic porcine mesenchymal stem cells (pMSCs; IBR-MSC; n=8), (2) implantation of an IBR loaded with media alone (IBR-Placebo; n=8), or (3) direct injection of 2.5×10^7 allogeneic pMSCs in the MI border zone (DI-MSC; n=6). Repeat cardiac MRI 4 weeks later was followed by IBR removal. Animals were survived for an additional 4-week "washout" phase then underwent a final cardiac MRI at 8 weeks after MI followed by invasive hemodynamics and necropsy.

and the IBR-Placebo group (−2.85±1.27 g; *P*=0.01); there was no significant difference between the groups (*P*=0.75; Figure 7A). When the components of LGE were analyzed separately, there was a significant decrease in core zone at 4 weeks (−6.38±1.45 g; *P*=0.01) and a significant increase in the gray zone extent (+2.39±0.46 g; *P*=0.01) in the IBR-MSC group. The IBR-Placebo group had a significant decrease in the core zone at 4 weeks (−3.46±1.10 g; *P*=0.01) but no significant change in the gray zone extent (+0.61±0.74 g; *P*=0.67). There was no significant difference between the groups for the change in core zone (*P*=0.25; Figure 7B), but there was for the gray zone (*P*=0.036; Figure 7C).

Bioreactor Removal and In Vitro Assessment of VEGF Release

After the 4-week MRI, IBRs were removed, washed, and placed in culture. Analysis of CM collected from outside recovered IBRs showed continued PF production by IBRs from the IBR-MSC group with a mean VEGF concentration of 786.9±256.6 pg/mL after 7 days in culture, indicating survival and continued PF production and release by allogeneic pMSCs after 4 weeks in vivo.

Washout Phase and 8-Week Cardiac MRI

Following IBR removal, animals remained in the study for an additional 4 week "washout" phase. The final cardiac MRI at 8 weeks after MI revealed that following the washout phase there were no significant differences for the changes in EDV (*P*=0.40), ESV (*P*=0.12), or LVEF (*P*=0.14; Figure 6) between the IBR-MSC and IBR-Placebo groups. Similarly, LGE MRI showed no significant differences between the groups in terms of the changes in the total scar size (*P*=0.42) or the separate core zone (*P*=0.82) and gray zone extent (*P*=0.91; Figure 7) following the washout phase.

Hemodynamic Assessment and Coronary Angiography

After the 8-week, final MRI, animals underwent invasive hemodynamics and coronary angiography. The mean dP/dT_{max} was 1182.2±185.8 mm Hg/s in the IBR-MSC group and 852.9±63.6 mm Hg/s in the IBR-Placebo group; this difference did not reach statistical significance (*P*=0.09). There were also no significant differences in measures of diastolic function, including dP/dT_{min} (−1706.5±185.8 mm Hg/s versus 1493.1±194.2 mm Hg/s; *P*=0.29) and tau (0.053±0.021 seconds versus 0.050±0.006 seconds; *P*=0.29). Coronary angiography revealed no significant difference in vessel patency of the left anterior descending artery (infarct vessel) between the groups, with Thrombolysis in Myocardial Infarction-3 (normal) flow in 6 of 8 (75%) of the IBR-MSC and 5 of 7 (71%) of the IBR-Placebo animals (*P*=NS).

Table. MRI Measurements

Measurement	IBR-MSC			IBR-Placebo			DI-MSC		
	Baseline	4 Weeks	8 Weeks	Baseline	4 Weeks	8 Weeks	Baseline	4 Weeks	8 Weeks
EDV, mL	90.37±6.06	90.71±5.24	103.71±7.40	85.11±4.07	95.48±6.84	104.00±10.06	76.55±4.13	103.62±15.2	114.80±11.17
ESV, mL	50.85±5.75	52.99±4.92	57.20±6.13	47.12±3.32	58.46±5.24	57.77±8.48	53.70±4.03	76.59±13.26	85.01±10.51
LVEF, %	44.64%±3.46	42.37±2.62	45.75%±2.70	44.54%±3.18	38.76%±3.37	45.69%±3.68	30.05±2.10	27.08±1.97	26.53±2.47
Core scar mass, g	19.54±2.87	13.16±1.90	13.46±2.05	16.70±2.56	13.23±2.24	14.06±2.22	16.42±0.86	12.71±1.18	12.05±0.84
Gray zone mass, g	3.06±0.55	5.46±0.71	6.65±0.69	5.05±0.50	5.66±0.79	6.92±1.15	4.98±1.71	3.26±0.56	4.24±0.51
LV mass, g	77.60±3.39	88.63±3.29	107.24±3.87	76.82±4.47	91.46±3.68	103.38±5.50	21.40±1.33	15.96±1.69	16.30±1.25

Mean values±standard error of the mean (SEM). DI indicates direct injection; EDV, end-diastolic volume; ESV, end-systolic volume; IBR, implantable bioreactor; LV, left ventricular; LVEF, left ventricular ejection fraction; MSC, mesenchymal stem cell.

Necropsy

On necropsy, 4 of 8 animals in the IBR-Placebo group had adherent pericardium, consistent with pericarditis, as compared with 0 of 8 animals in the IBR-MSC group (P=0.02). Gross inspection of the lungs, liver, kidneys, and spleen revealed no evidence of neoplasm in either group. All animals (16/16) who underwent baseline MRI and IBR implantation survived the full duration of the 8-week study.

Histology

Histologic comparison of the infarct border zone from IBR-MSC and IBR-Placebo animals at 8 weeks using hematoxylin and eosin and Masson's trichrome revealed the MRI gray zone correlated with areas of heterogenous tissue composed of myocytes intermixed with fibrotic scar at the infarct border zone (see Figure 7E).

Comparison With DI MSCs

Of the 6 animals that underwent DI of 25 million MSCs, all survived the injection procedure performed 3 days after MI, although 1 was euthanized in the week after DI because of failure to thrive. The remaining 5 animals survived the duration of the study. Cardiac MRI at 4 weeks following DI revealed large-magnitude, although statistically nonsignificant, changes compared with baseline for EDV (+27.07±12.17 mL; P=0.08), ESV (+22.89±9.39 mL, P=0.08), and LVEF (−2.97±1.33; P=0.08) on paired analyses. When the 3 groups (IBR-MSC, IBR-Placebo, and DI-MSC) were compared, there were significant differences across the 3 groups for the change in ESV (P=0.05). Post hoc analysis revealed that the change in ESV at 4 weeks was significantly lower in the IBR-MSC group than the DI-MSC group (+2.14±4.13 mL versus +22.89±9.39 mL; P=0.01). For the change in EDV at 4 weeks, the difference across the 3 groups did not reach significance (P=0.06). There was also no significant difference across the 3 groups for change in LVEF (P=0.51).

The MRI LGE studies at 4 weeks demonstrated significant decreases in total scar (−5.44±1.43 g; P=0.04) and core scar (−3.72±1.55 g; P=0.04) extents in the DI-MSC group compared with baseline, but no significant change in gray zone extent (−1.72±1.46 g; P=0.35). Across the 3 groups, there was a significant difference for the change in gray zone extent (P=0.016), with post hoc analysis revealing a greater increase in gray zone in the IBR-MSC group than in the DI-MSC group (+2.39±0.46 g versus −1.72±1.46 g, P=0.003). There was no difference for the change in gray zone extent between the IBR-Placebo and DI-MSC groups (P=0.11), and

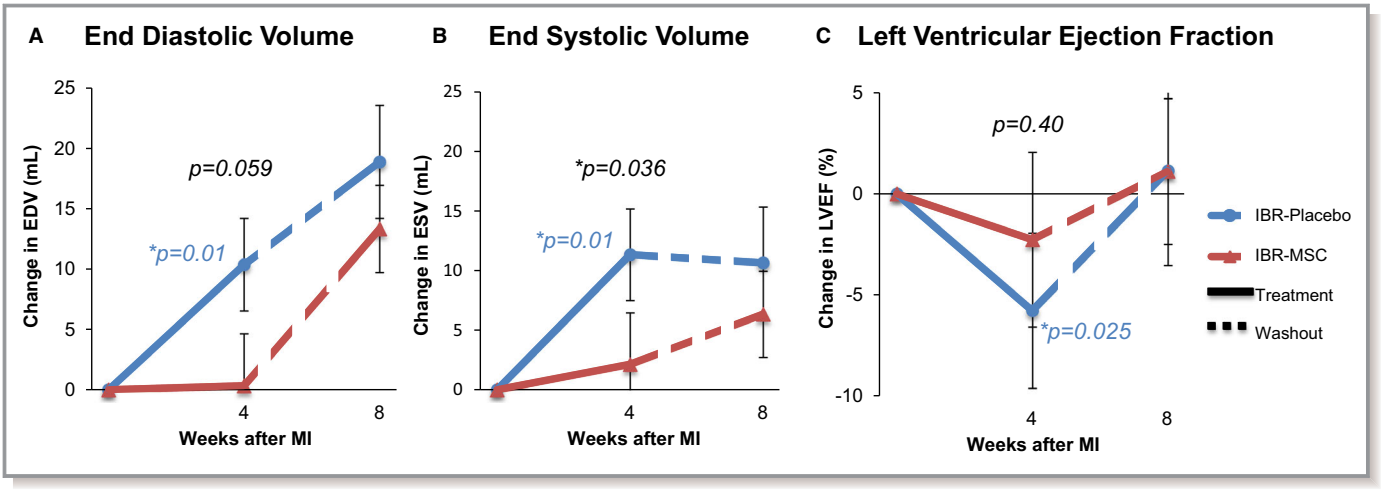

Figure 6. Implantable bioreactor (IBR) based cell therapy prevents adverse remodeling compared with placebo at 4 weeks after myocardial infarction as assessed by MRI. Over the 4-week treatment phase, end-diastolic volume (EDV) (**A**) and end-systolic volume (ESV) (**B**) significantly increased in the IBR-Placebo group, but not in the IBR-mesenchymal stem cell (MSC) group. These changes were accompanied by a significant decrease in left ventricular ejection fraction (LVEF) in the IBR-Placebo group but not in the IBR-MSC group (**C**). Unpaired analysis demonstrated a significant difference for ESV (P=0.036), but not EDV (P=0.059) or LVEF (P=0.40) between the 2 groups at 4 weeks. After the final 4-week "washout" phase following IBR removal (dashed lines), animals in the IBR-MSC group were no longer protected from adverse remodeling, with no significant difference between groups for the changes in EDV, ESV, or LVEF. Colored P values indicate significant differences for paired analyses where present. Black P values show results of unpaired analyses at 4 weeks; there were no significant differences between the groups from week 4 to 8 (P values not shown). *indicate p-values less than or equal to 0.05. P-values that are greater than 0.05 do not have an asterisk.

also no significant difference across the 3 groups for the change in total scar mass (P=0.39) and core zone mass (P=0.33) at 4 weeks.

Necropsy at 8 weeks revealed no evidence of pericarditis in the DI-MSC animals that survived the duration of the study (0/5).

Discussion

There is growing evidence that the beneficial effects of stem cell administration following MI are mediated to a large extent by PFs, including growth factors and cytokines, as opposed to cell engraftment.[9–12] Here, we present proof-of-concept that a device designed to harness the beneficial effects of stem cell PFs by providing a protected environment in the vascular space, remote from the heart, from which exogenous allogeneic stem cells can release PFs over a prolonged period while being protected from washout, dilution, and immune-mediated rejection. Our findings suggest that allogeneic MSCs deployed in an IBR device can reduce adverse cardiac remodeling 4 weeks after MI compared with both placebo and the same number of directly injected MSCs. By nature of the IBR design, which allows free release of PFs but not cells, the beneficial effects observed in the IBR-MSC group are necessarily not the result of stem cell engraftment or direct cell-cell interaction, and thus provide further evidence to support the "paracrine hypothesis" of stem cell–mediated cardiac repair.[9,10]

Specifically, we show that in a large animal model, the deployment and maintenance of a catheter-based IBR in the superior vena cava with contained exogenous stem cells is feasible and well tolerated for up to 4 weeks with no evidence of adverse effects from the IBR itself or from the contained cells. This is despite the fact that the cells used were xenogeneic in the preliminary biocompatibility testing, when IBRs containing human MSCs were implanted in pigs, and allogeneic in the MI efficacy study, when IBRs loaded with pig MSCs were deployed in unrelated pigs. Second, we show that a relatively small number of MSCs (2.5×10^7) contained in the IBR in a location remote from the heart exerts protective effects as evidenced by decreased adverse remodeling and preserved LVEF over 4 weeks following an MI. The magnitude of this benefit was significant, including a >5-fold difference in the change in ESV compared with placebo (+2.14 mL versus +11.35 mL; P=0.036). This result compares favorably with those reported in clinical trials of angiotensin-converting enzyme inhibitors,[24,25] which are currently first-line therapy to limit adverse remodeling and left ventricular dysfunction after MI.[26] These results also compare favorably with clinical trials of bone marrow–derived stem cells in acute MI, despite the use of much higher numbers of cells in those studies.[27,28] In this study, there was a significantly greater increase in ESV 4 weeks after MI in animals receiving intramyocardial injection of 25 million MSCs compared with the same number of cells deployed in the IBR. Relative to prior animal studies, 25 million MSCs is a low dose,[29–31] and our results suggest

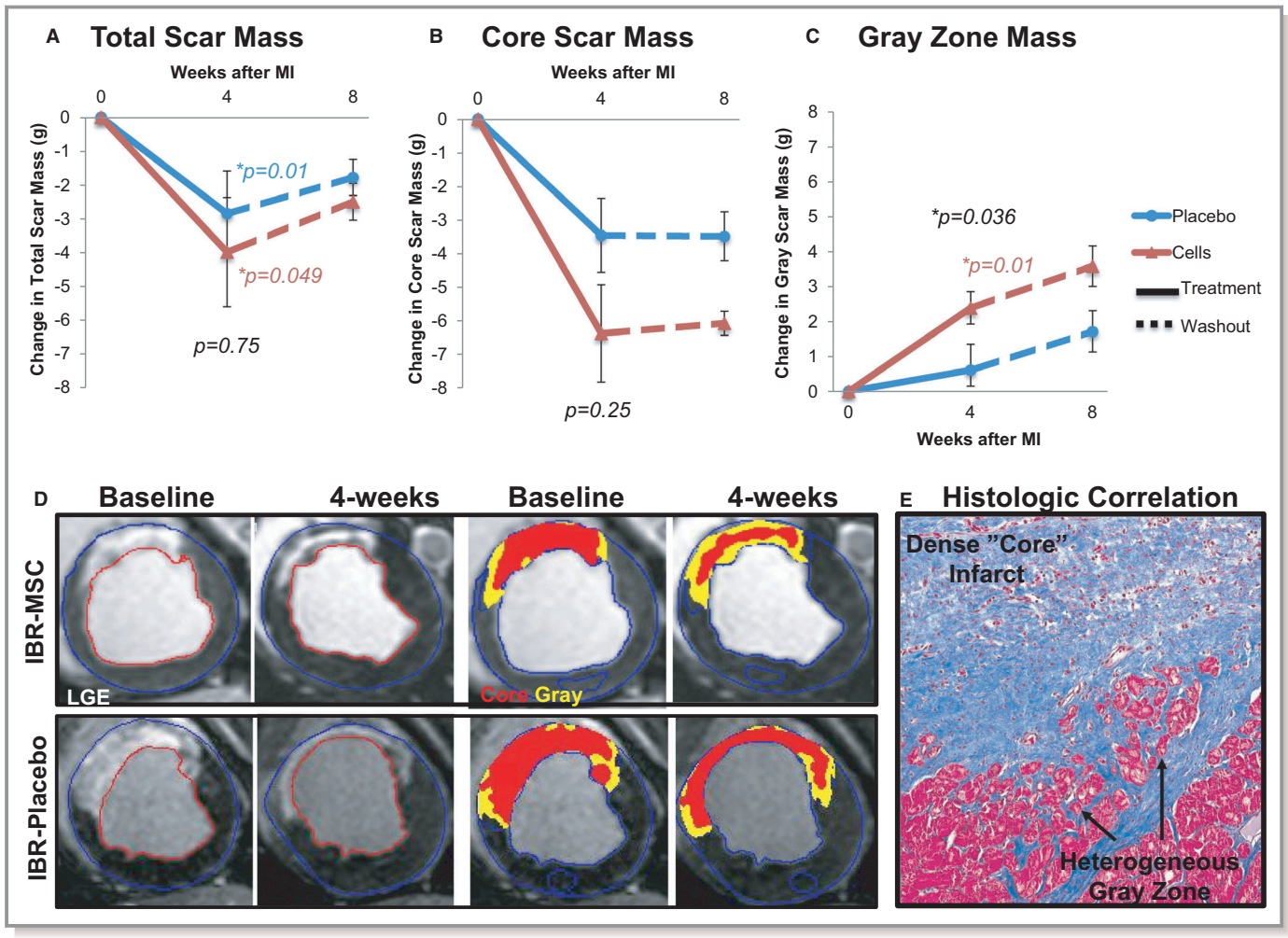

Figure 7. Change in infarct mass. Total infarct mass assessed by late gadolinium-enhanced (LGE) MRI significantly decreased in both the implantable bioreactor mesenchymal stem cell (IBR-MSC) and IBR-Placebo groups over the 4 weeks following implantation (**A**). Over the same period, dense "core" zone mass decreased significantly in both groups, although the magnitude was greater in the IBR-MSC than in the IBR-Placebo group (−6.38 g vs −3.46 g) (**B**). This decrease in core mass was accompanied by a significant increase in the heterogeneous peri-infarct "gray" zone in the IBR-MSC but not in the IBR-Placebo animals (**C**). During the 4-week "washout" phase following IBR removal (dashed lines), there were no significant differences in scar size change between the groups. Colored *P* values indicate significant differences for paired analyses where present. Black *P* values show results of unpaired analyses at 4 weeks; there were no significant differences between the groups from weeks 4 to 8 (*P* values not shown). Representative images of LGE extent at baseline and 4 weeks along with quantification of core (red) and peri-infarct gray zone (yellow) masses are shown (**D**). Masson's trichrome stain of the infarct border zone corresponding to the MRI gray zone revealed heterogeneous tissue containing viable myocytes intermixed with scar tissue (**E**).

that while this dose is sufficient to protect against adverse remodeling when deployed in the IBR, intramyocardial injection requires higher numbers of MSCs to protect against adverse remodeling.

The observed attenuation of adverse remodeling in animals in the IBR-MSC group was accompanied by differential tissue characteristics within the infarct as assessed by LGE. At week 4, there was a significant increase in the heterogeneous gray zone extent in the IBR-MSC group that was not observed in the IBR-Placebo or DI-MSC groups. Histology at 8 weeks after MI revealed the MRI gray zone corresponded with heterogenous tissue composed of viable myocytes and scar tissue (see Figure 7E). The peri-infarct border zone is thought to be important in remodeling because of the presence of myocytes prone to apoptosis and dedifferentiation.[32,33] The significant increase in MRI gray zone in the IBR-MSC group suggests improved salvage of viable myocytes in the peri-infarct border zone and/or prevention of their dedifferentiation and apoptosis.

In addition, there was a marked difference in the prevalence of pericarditis observed between the IBR-MSC and IBR-Placebo groups at the time of necropsy: 0% versus 50% (*P*=0.02). Pericarditis after MI is typically present following large infarcts and may result from a robust inflammatory response.[34,35] Inflammation following MI that is prolonged,

excessive in magnitude, and/or insufficiently suppressed can lead to sustained tissue damage, promoting adverse remodeling and resultant heart failure.[36,37] The absence of pericarditis in the IBR-MSC group suggests modulation of inflammation, which is a known effect of MSCs attributable to the release of soluble factors.[38–41] There was also no evidence of pericarditis in the DI-MSC group, consistent with the anti-inflammatory effects of MSCs. That both the IBR-MSC and DI-MSC groups were protected from pericarditis, but only the IBR-MSC from adverse remodeling suggests that the early, time-limited anti-inflammatory effect of DI-MSCs may be sufficient to prevent pericarditis, but that sustained PF release is necessary to prevent remodeling.

While further study is needed, the protection from adverse remodeling and increase in the peri-infarct heterogeneous gray zone observed in the IBR-MSC group appear to be directly related to the presence of the IBR-MSC device, as over the 4-week "washout" phase after IBR removal there was no significant difference between the IBR-MSC and IBR-Placebo groups in terms of protection from further adverse remodeling or change in infarct size and composition. As a proof-of-concept study, the parameters tested here were limited in terms of the initiation and duration of IBR placement and of the number and type of cells used. In future studies, it will be important to examine these factors. For example, there are clinical data to suggest that delaying cell delivery by several days after MI enhances the benefit, likely due in part to poor cell survival in the inhospitable, proinflammatory environment of recently infarcted myocardium.[42] In contrast, angiotensin-converting enzyme inhibitor administration is most effective when initiated early, that is, in the first 24 to 48 hours following an MI.[25,26] Intravascular bioreactor-based therapy is predicated on the provision of a protected environment for contained cells in a location remote from the heart, and thus could afford a mechanism to provide the benefit of cell-based PF administration throughout the time course of infarct healing, including shortly after MI when the anti-inflammatory and antiapoptotic effects of stem cell PFs would be expected to be advantageous. Importantly, the IBR can be readily placed in acutely ill patients with the same techniques used to place a central venous line and without the potential risks associated with more invasive cell delivery techniques in the early post-MI phase. In addition, while most cell death and inflammation occur in the initial days after MI, adverse remodeling is known to continue for weeks to months.[1,43–45] Analysis of the media collected from outside of the MSC-IBRs explanted after 4 weeks in vivo showed continued VEGF production, indicating survival and continued PF release by the contained MSCs. As such, if an IBR were left in place for longer than 4 weeks, further protection from adverse remodeling may be afforded, perhaps resulting in a more durable effect.

The dose and type of cells deployed in the IBR also requires further study. The dose of 2.5×10^7 MSCs used in this study was chosen on the basis of a limited assessment of in vitro PF production for a relatively simple IBR design and geometry. The IBR could be designed to accommodate a much larger number of cells and allow for dose efficacy studies to determine the optimal in vivo cell dose. Also, while MSCs were used here, other cell types may have a favorable PF profile for cardiac repair,[11,12] and the protected, immune-privileged environment the IBR provides could allow for use of multiple different cell types, whether allogeneic or xenogeneic, alone, or in combinations. Deployment of the IBR via the internal jugular vein, as tested here, would also provide ready access to replace or "recharge" the contained cells, as there is evidence that repeat dosing of stem cells may be advantageous.[46]

Finally, an alternate strategy would be to deliver PFs alone. However, it remains unclear which of the hundreds or perhaps thousands of PFs produced by stem cells are critical for cardiac repair, whether optimal action requires a combination of particular factors, and how the ratios and types of factors vary over the time course of the healing process. This may explain why the results of clinical trials employing individual PFs administered to the heart or peripheral vasculature did not, to date, achieve all of the desired benefits.[47–50] In contrast, delivery of an IBR containing cells that have the ability to produce their full complement of PFs and vary their release based on changing environmental conditions would, in theory, allow the contained cells to tailor the combination of factors released to optimize tissue repair and healing.

Study Limitations

The conclusions from this study are limited by the relatively small number of animals studied (n=8 in each IBR group and n=6 in the DI group). In addition, the animals were young and healthy, and thus may not be indicative of clinical conditions in which patients suffering an MI are typically older with concomitant conditions such as diabetes mellitus and hypertension that may adversely affect recovery and remodeling. The animals in this study were also not treated with the evidence-based medical therapies (eg, angiotensin-converting enzyme inhibitors and beta-blockers) that postinfarction patients typically receive. In addition, although we provide data indicating that MSCs release PFs from the IBR in vitro and continue to do so after being explanted from the body, we were unable to obtain in vivo measures of PF release because of an inability to differentiate IBR-released PFs from endogenous PFs attributable in part to a limited number of porcine-specific PF antibodies. We also cannot identify which PFs resulted in the beneficial effect noted in the IBR-MSC group. While we show that porcine MSCs contained in explanted

IBRs continued to release VEGF in vitro, this factor may not be representative of the many PFs released by MSCs. Likewise, while a significant reduction in pericarditis was seen in the IBR-MSC group compared with placebo, we did not collect serum samples to correlate this result to inflammatory markers such as interleukin-1, interleukin-6, or tumor necrosis factor-alpha. Finally, the hemodynamic and autopsy data were obtained from animals at 8 weeks after MI, which was 4 weeks after removal of the IBR. As a result, we do not have hemodynamic or pathologic data at 4 weeks after MI, when the favorable MRI remodeling effects were most pronounced, and thus are limited in our ability to correlate the hemodynamic and pathologic findings reported here with the observed beneficial effects on adverse remodeling.

Conclusions

In summary, we demonstrate here proof of concept that allogeneic MSCs, housed in the protected environment of an IBR in the superior vena cava, remote from the heart, can prevent adverse remodeling and alter scar composition after MI compared with placebo and to direct myocardial injection of the same number of MSCs. The IBR allows free release of soluble PFs but not of cells, and thus the beneficial effects observed in the IBR-MSC group are necessarily mediated by paracrine mechanisms as opposed to stem cell engraftment, lending further support to the paracrine hypothesis of myocardial repair that underlies this therapeutic paradigm.

Acknowledgments

We thank José Rodriguez for assistance with the MRI studies and Marcos Rosado for assistance with the animal procedures.

Sources of Funding

This work was funded by a grant from the Johns Hopkins University School of Medicine's The Magic That Matters Fund, a gift to the Johns Hopkins University School of Medicine Division of Cardiology from the Zegar Family Foundation, and support from the Clarence Doodeman Endowment in Cardiology.

Disclosures

This study involves technology that was developed at the Johns Hopkins University and is under license by Domicell, Inc. Drs Johnston, Hwang, Schulman, Tomaselli, Weiss, and Gerstenblith are inventors of the technology. Additionally, they are founders of Domicell and hold equity in the company. Johns Hopkins University also holds equity in Domicell. This arrangement has been reviewed and approved by Johns Hopkins University in accordance with its conflict of interest policies. Ms Bogdan is an employee of Domicell, Inc. Dr Hare reports having a patent for cardiac cell–based therapy and holds equity in Vestion Inc. He maintains a professional relationship with Vestion Inc. as a consultant and member of the Board of Directors and Scientific Advisory Board. Vestion Inc. did not play a role in the design and conduct of the study. Dr Hare holds a relationship with Longeveron, LLC that includes consulting and member of the Board of Directors and Scientific Advisory Board. The remaining authors have no disclosures to report.

References

1. Pfeffer MA, Braunwald E. Ventricular remodeling after myocardial infarction. Experimental observations and clinical implications. *Circulation*. 1990;81:1161–1172.
2. White HD, Norris RM, Brown MA, Brandt PW, Whitlock RM, Wild CJ. Left ventricular end-systolic volume as the major determinant of survival after recovery from myocardial infarction. *Circulation*. 1987;76:44–51.
3. Chavakis E, Koyanagi M, Dimmeler S. Enhancing the outcome of cell therapy for cardiac repair: progress from bench to bedside and back. *Circulation*. 2010;121:325–335.
4. Sanganalmath SK, Bolli R. Cell therapy for heart failure: a comprehensive overview of experimental and clinical studies, current challenges, and future directions. *Circ Res*. 2013;113:810–834.
5. Gouadon E, Moore-Morris T, Smit NW, Chatenoud L, Coronel R, Harding SE, Jourdon P, Lambert V, Rucker-Martin C, Pucéat M. Concise review: pluripotent stem cell-derived cardiac cells, a promising cell source for therapy of heart failure: where do we stand? *Stem Cells*. 2016;34:34–43.
6. Yanamandala M, Zhu W, Garry DJ, Kamp TJ, Hare JM, Jun HW, Yoon YS, Bursac N, Prabhu SD, Dorn GW, Bolli R, Kitsis RN, Zhang J. Overcoming the roadblocks to cardiac cell therapy using tissue engineering. *J Am Coll Cardiol*. 2017;70:766–775.
7. Robey TE, Saiget MK, Reinecke H, Murry CE. Systems approaches to preventing transplanted cell death in cardiac repair. *J Mol Cell Cardiol*. 2008;45:567–581.
8. Terrovitis J, Lautamaki R, Bonios M, Fox J, Engles JM, Yu J, Leppo MK, Pomper MG, Wahl RL, Seidel J, Tsui BM, Bengel FM, Abraham MR, Marban E. Noninvasive quantification and optimization of acute cell retention by in vivo positron emission tomography after intramyocardial cardiac-derived stem cell delivery. *J Am Coll Cardiol*. 2009;54:1619–1626.
9. Gnecchi M, Zhang Z, Ni A, Dzau VJ. Paracrine mechanisms in adult stem cell signaling and therapy. *Circ Res*. 2008;103:1204–1219.
10. Chimenti I, Smith RR, Li TS, Gerstenblith G, Messina E, Giacomello A, Marban E. Relative roles of direct regeneration versus paracrine effects of human cardiosphere-derived cells transplanted into infarcted mice. *Circ Res*. 2010;106:971–980.
11. Li TS, Cheng K, Malliaras K, Smith RR, Zhang Y, Sun B, Matsushita N, Blusztajn A, Terrovitis J, Kusuoka H, Marban L, Marban E. Direct comparison of different stem cell types and subpopulations reveals superior paracrine potency and myocardial repair efficacy with cardiosphere-derived cells. *J Am Coll Cardiol*. 2012;59:942–953.
12. Tseliou E, Fouad J, Reich H, Slipczuk L, de Couto G, Aminzadeh M, Middleton R, Valle J, Weixin L, Marban E. Fibroblasts rendered antifibrotic, antiapoptotic, and angiogenic by priming with cardiosphere-derived extracellular membrane vesicles. *J Am Coll Cardiol*. 2015;66:599–611.
13. Comite P, Cobianchi L, Avanzini MA, Zonta S, Mantelli M, Achille V, De Martino M, Cansolino L, Ferrari C, Alessiani M, Maccario R, Gandolfo GM, Dionigi P, Locatelli F, Bernardo ME. Isolation and ex vivo expansion of bone marrow-derived porcine mesenchymal stromal cells: potential for application in an experimental model of solid organ transplantation in large animals. *Transplant Proc*. 2010;42:1341–1343.
14. Peterbauer-Scherb A, van Griensven M, Meinl A, Gabriel C, Redl H, Wolbank S. Isolation of pig bone marrow mesenchymal stem cells suitable for one-step procedures in chondrogenic regeneration. *J Tissue Eng Regen Med*. 2010;4:485–490.

15. Pittenger MF. Mesenchymal stem cells from adult bone marrow. *Methods Mol Biol*. 2008;449:27–44.
16. Hwang CW, Johnston PV, Gerstenblith G, Weiss RG, Tomaselli GF, Bogdan VE, Panigrahi A, Leszczynska A, Xia Z. Stem cell impregnated nanofiber stent sleeve for on-stent production and intravascular delivery of paracrine factors. *Biomaterials*. 2015;52:318–326.
17. Duffy GP, D'Arcy S, Ahsan T, Nerem RM, O'Brien T, Barry F. Mesenchymal stem cells overexpressing ephrin-b2 rapidly adopt an early endothelial phenotype with simultaneous reduction of osteogenic potential. *Tissue Eng Part A*. 2010;16:2755–2768.
18. Johnston PV, Sasano T, Mills K, Evers R, Lee ST, Smith RR, Lardo AC, Lai S, Steenbergen C, Gerstenblith G, Lange R, Marban E. Engraftment, differentiation, and functional benefits of autologous cardiosphere-derived cells in porcine ischemic cardiomyopathy. *Circulation*. 2009;120:1075–1083.
19. Sasano T, McDonald AD, Kikuchi K, Donahue JK. Molecular ablation of ventricular tachycardia after myocardial infarction. *Nat Med*. 2006;12:1256–1258.
20. Martelli A, Berardinelli P, Russo V, Mauro A, Bernabo N, Gioia L, Mattioli M, Barboni B. Spatio-temporal analysis of vascular endothelial growth factor expression and blood vessel remodelling in pig ovarian follicles during the periovulatory period. *J Mol Endocrinol*. 2006;36:107–119.
21. Schmidt A, Azevedo CF, Cheng A, Gupta SN, Bluemke DA, Foo TK, Gerstenblith G, Weiss RG, Marban E, Tomaselli GF, Lima JA, Wu KC. Infarct tissue heterogeneity by magnetic resonance imaging identifies enhanced cardiac arrhythmia susceptibility in patients with left ventricular dysfunction. *Circulation*. 2007;115:2006–2014.
22. Wu KC, Gerstenblith G, Guallar E, Marine JE, Dalal D, Cheng A, Marban E, Lima JA, Tomaselli GF, Weiss RG. Combined cardiac magnetic resonance imaging and C-reactive protein levels identify a cohort at low risk for defibrillator firings and death. *Circ Cardiovasc Imaging*. 2012;5:178–186.
23. Karantalis V, Suncion-Loescher VY, Bagno L, Golpanian S, Wolf A, Sanina C, Premer C, Kanelidis AJ, McCall F, Wang B, Balkan W, Rodriguez J, Rosado M, Morales A, Hatzistergos K, Natsumeda M, Margitich I, Schulman IH, Gomes SA, Mushtaq M, DiFede DL, Fishman JE, Pattany P, Zambrano JP, Heldman AW, Hare JM. Synergistic effects of combined cell therapy for chronic ischemic cardiomyopathy. *J Am Coll Cardiol*. 2015;66:1990–1999.
24. Pfeffer MA, Lamas GA, Vaughan DE, Parisi AF, Braunwald E. Effect of captopril on progressive ventricular dilatation after anterior myocardial infarction. *N Engl J Med*. 1988;319:80–86.
25. Sharpe N, Smith H, Murphy J, Greaves S, Hart H, Gamble G. Early prevention of left ventricular dysfunction after myocardial infarction with angiotensin-converting-enzyme inhibition. *Lancet*. 1991;337:872–876.
26. O'Gara PT, Kushner FG, Ascheim DD, Casey DE Jr, Chung MK, de Lemos JA, Ettinger SM, Fang JC, Fesmire FM, Franklin BA, Granger CB, Krumholz HM, Linderbaum JA, Morrow DA, Newby LK, Ornato JP, Ou N, Radford MJ, Tamis-Holland JE, Tommaso CL, Tracy CM, Woo YJ, Zhao DX, Anderson JL, Jacobs AK, Halperin JL, Albert NM, Brindis RG, Creager MA, DeMets D, Guyton RA, Hochman JS, Kovacs RJ, Kushner FG, Ohman EM, Stevenson WG, Yancy CW; American College of Cardiology Foundation/American Heart Association Task Force on Practice Guidelines. 2013 ACCF/AHA guideline for the management of ST-elevation myocardial infarction: a report of the American College of Cardiology Foundation/American Heart Association Task Force on Practice Guidelines. *Circulation*. 2013;127:e362–e425.
27. Delewi R, Hirsch A, Tijssen JG, Schachinger V, Wojakowski W, Roncalli J, Aakhus S, Erbs S, Assmus B, Tendera M, Goekmen Turan R, Corti R, Henry T, Lemarchand P, Lunde K, Cao F, Huikuri HV, Surder D, Simari RD, Janssens S, Wollert KC, Plewka M, Grajek S, Traverse JH, Zijlstra F, Piek JJ. Impact of intracoronary bone marrow cell therapy on left ventricular function in the setting of ST-segment elevation myocardial infarction: a collaborative meta-analysis. *Eur Heart J*. 2014;35:989–998.
28. Hare JM, Traverse JH, Henry TD, Dib N, Strumpf RK, Schulman SP, Gerstenblith G, DeMaria AN, Denktas AE, Gammon RS, Hermiller JB Jr, Reisman MA, Schaer GL, Sherman W. A randomized, double-blind, placebo-controlled, dose-escalation study of intravenous adult human mesenchymal stem cells (prochymal) after acute myocardial infarction. *J Am Coll Cardiol*. 2009;54:2277–2286.
29. Amado LC, Saliaris AP, Schuleri KH, St John M, Xie JS, Cattaneo S, Durand DJ, Fitton T, Kuang JQ, Stewart G, Lehrke S, Baumgartner WW, Martin BJ, Heldman AW, Hare JM. Cardiac repair with intramyocardial injection of allogeneic mesenchymal stem cells after myocardial infarction. *Proc Natl Acad Sci U S A*. 2005;102:11474–11479.
30. Schuleri KH, Amado LC, Boyle AJ, Centola M, Saliaris AP, Gutman MR, Hatzistergos KE, Oskouei BN, Zimmet JM, Young RG, Heldman AW, Lardo AC, Hare JM. Early improvement in cardiac tissue perfusion due to mesenchymal stem cells. *Am J Physiol Heart Circ Physiol*. 2008;294:H2002–H2011.
31. Bharti D, Shivakumar SB, Subbarao RB, Rho GJ. Research advancements in porcine derived mesenchymal stem cells. *Curr Stem Cell Res Ther*. 2016;11:78–93.
32. Musialek P, Tekieli L, Kostkiewicz M, Miszalski-Jamka T, Klimeczek P, Mazur W, Szot W, Majka M, Banys RP, Jarocha D, Walter Z, Krupinski M, Pieniazek P, Olszowska M, Zmudka K, Pasowicz M, Kereiakes DJ, Tracz W, Podolec P, Wojakowski W. Infarct size determines myocardial uptake of $CD34^+$ cells in the peri-infarct zone: results from a study of (99m)Tc-extametazime-labeled cell visualization integrated with cardiac magnetic resonance infarct imaging. *Circ Cardiovasc Imaging*. 2013;6:320–328.
33. Abbate A, Bussani R, Biondi-Zoccai GG, Santini D, Petrolini A, De Giorgio F, Vasaturo F, Scarpa S, Severino A, Liuzzo G, Leone AM, Baldi F, Sinagra G, Silvestri F, Vetrovec GW, Crea F, Biasucci LM, Baldi A. Infarct-related artery occlusion, tissue markers of ischaemia, and increased apoptosis in the peri-infarct viable myocardium. *Eur Heart J*. 2005;26:2039–2045.
34. Dressler W. The postmyocardial infarction syndrome; recurrent pericarditis, pleurisy, and pneumonitis. *Heart Bull*. 1958;7:102–104.
35. Imazio M, Hoit BD. Post-cardiac injury syndromes. An emerging cause of pericardial diseases. *Int J Cardiol*. 2013;168:648–652.
36. Prabhu SD, Frangogiannis NG. The biological basis for cardiac repair after myocardial infarction: from inflammation to fibrosis. *Circ Res*. 2016;119:91–112.
37. Kempf T, Zarbock A, Vestweber D, Wollert KC. Anti-inflammatory mechanisms and therapeutic opportunities in myocardial infarct healing. *J Mol Med (Berl)*. 2012;90:361–369.
38. Aggarwal S, Pittenger MF. Human mesenchymal stem cells modulate allogeneic immune cell responses. *Blood*. 2005;105:1815–1822.
39. Prockop DJ, Oh JY. Mesenchymal stem/stromal cells (MSCs): role as guardians of inflammation. *Mol Ther*. 2012;20:14–20.
40. D'souza N, Rossignoli F, Golinelli G, Grisendi G, Spano C, Candini O, Osturu S, Catani F, Paolucci P, Horwitz EM, Dominici M. Mesenchymal stem/stromal cells as a delivery platform in cell and gene therapies. *BMC Med*. 2015;13:186.
41. Yao Y, Huang J, Geng Y, Qian H, Wang F, Liu X, Shang M, Nie S, Liu N, Du X, Dong J, Ma C. Paracrine action of mesenchymal stem cells revealed by single cell gene profiling in infarcted murine hearts. *PLoS One*. 2015;10:e0129164.
42. Schachinger V, Erbs S, Elsasser A, Haberbosch W, Hambrecht R, Holschermann H, Yu J, Corti R, Mathey DG, Hamm CW, Suselbeck T, Assmus B, Tonn T, Dimmeler S, Zeiher AM. Intracoronary bone marrow-derived progenitor cells in acute myocardial infarction. *N Engl J Med*. 2006;355:1210–1221.
43. Fishbein MC, Maclean D, Maroko PR. The histopathologic evolution of myocardial infarction. *Chest*. 1978;73:843–849.
44. Hutchins GM, Bulkley BH. Infarct expansion versus extension: two different complications of acute myocardial infarction. *Am J Cardiol*. 1978;41:1127–1132.
45. Pfeffer JM, Pfeffer MA, Braunwald E. Influence of chronic captopril therapy on the infarcted left ventricle of the rat. *Circ Res*. 1985;57:84–95.
46. Tang XL, Nakamura S, Li Q, Wysoczynski M, Gumpert AM, Wu WJ, Hunt G, Stowers H, Ou Q, Bolli R. Repeated administrations of cardiac progenitor cells are superior to a single administration of an equivalent cumulative dose. *J Am Heart Assoc*. 2018;7:e007400. DOI: 10.1161/JAHA.117.007400.
47. Kastrup J, Jorgensen E, Ruck A, Tagil K, Glogar D, Ruzyllo W, Botker HE, Dudek D, Drvota V, Hesse B, Thuesen L, Blomberg P, Gyongyosi M, Sylven C; Euroinject One G. Direct intramyocardial plasmid vascular endothelial growth factor-A165 gene therapy in patients with stable severe angina pectoris a randomized double-blind placebo-controlled study: the Euroinject One trial. *J Am Coll Cardiol*. 2005;45:982–988.
48. Stewart DJ, Kutryk MJ, Fitchett D, Freeman M, Camack N, Su Y, Della Siega A, Bilodeau L, Burton JR, Proulx G, Radhakrishnan S; NORTHERN Trial Investigators. VEGF gene therapy fails to improve perfusion of ischemic myocardium in patients with advanced coronary disease: results of the NORTHERN trial. *Mol Ther*. 2009;17:1109–1115.
49. Kusumanto YH, van Weel V, Mulder NH, Smit AJ, van den Dungen JJ, Hooymans JM, Sluiter WJ, Tio RA, Quax PH, Gans RO, Dullaart RP, Hospers GA. Treatment with intramuscular vascular endothelial growth factor gene compared with placebo for patients with diabetes mellitus and critical limb ischemia: a double-blind randomized trial. *Hum Gene Ther*. 2006;17:683–691.
50. Belch J, Hiatt WR, Baumgartner I, Driver IV, Nikol S, Norgren L, Van Belle E; TAMARIS Committees and Investigators. Effect of fibroblast growth factor NV1FGF on amputation and death: a randomised placebo-controlled trial of gene therapy in critical limb ischaemia. *Lancet*. 2011;377:1929–1937.